

Supporting Information

To

Brønsted Acid Sites of Zeolitic Strength in Amorphous Silica-Alumina

Emiel J.M. Hensen,* Dilip G. Poduval, J.A. Rob van Veen, and Marcello S. Rigutto

1. Materials

For validation of the hydrogen-deuterium (H/D) exchange FTIR method, a faujasite zeolite with a silica to alumina ratio (SAR) of 9.6 was used. This zeolite was obtained through treatment of a faujasite zeolite with $(\text{NH}_4)_2\text{SiF}_6$, which replaces part of the framework aluminium by silicon^[1] and produces a material largely free of extraframework aluminium (^{27}Al NMR: fraction $\text{Al}^{\text{IV}} = 97\%$). H/D exchange FTIR was employed to steam stabilized zeolites, clays and amorphous silica-aluminas: five steam stabilized faujasite zeolites with SAR = 8.1-33.1 (Zeolyst International) and one saponite clay (a Mg-saponite prepared according to the method by Vogels et al.^[2]) with SAR = 13. ASAs prepared by homogeneous deposition of aluminium on silica. The samples are denoted by ASA($X/Y, T$), where X and Y refer to the alumina and silica contents by weight and T refers to the calcination temperature.^[3] Control experiments were carried out with silica (SiO_2 , Sipernat 50) and γ -alumina (Ketjen CK-300). An industrial ASA reference sample (55 wt% Al_2O_3) prepared by grafting aluminium to in situ prepared silica-gel at pH 3 was used as received. This ASA was calcined at 773 K and 1073 K. Na-ASA was obtained by stirring an amount of ASA(5/95, 1073) with a 2 M sodium acetate solution for 1 h. After filtration, the ASA was washed three times with a 4 mM sodium acetate solution, before drying in a stove at 383 K overnight.

2. H/D exchange FT infrared spectroscopy

H/D exchange of hydroxyl groups with perdeuterated benzene was followed in situ by infrared spectroscopy. Infrared spectra were recorded in transmission mode in a Bruker IFS-113v FTIR spectrometer. Typically, a powdered aluminosilicate sample was pressed into a self-supporting wafer with a density $\rho = 9 \text{ mg/cm}^2$ and placed in an in situ cell. After calcining the catalyst wafer at 823 K, the catalyst was evacuated to a pressure better than

2×10^{-6} mbar and temperature was lowered to 303 K. A background spectrum was recorded. Perdeuterobenzene (C_6D_6 , Merck, purity 99.96 %) was introduced into the cell from a glass ampoule. The total volume of C_6D_6 administered to the cell was $0.33 \text{ mmol} \pm 1\%$, resulting in a pressure of 10 mbar. The sample was exposed to perdeuterobenzene for 10 s followed by evacuation for 30 min. Then, a next spectrum of the partially exchanged sample was recorded. This sequence was automatically repeated with exposure times of 30 s, 5 min, 10 min, 20 min, 30 min at 303 K, 30 min at 323 K, 30 min at 353 K, 30 min at 373 K, 30 min at 423 K and 30 min at 523 K. For each spectrum, 125 scans were accumulated at a resolution of 2 cm^{-1} . Difference spectra were obtained by subtracting the initial spectrum of the dehydrated sample from the spectra after exposure to C_6D_6 .

3. Validation of method for an ultrastabilized Y zeolite

It was first established that the non-acidic hydroxyl groups in silica and γ -alumina do not exchange during H/D exchange up to 353 K. The H/D exchange FTIR method was validated for a zeolite with a silica-to-alumina ratio of 9.6 with nearly all aluminium in framework positions. The IR spectrum of the dehydrated zeolite in Fig. S1a shows three bands. Two bands at 3626 cm^{-1} and 3550 cm^{-1} are due to acid sites in the supercages (the high-frequency HF band) and in the smaller cages (the low frequency LF band), respectively. The third band is due to silanol groups on the external zeolite surface (3743 cm^{-1}). After progressive H/D exchange at 323 K, nearly all Bronsted acid sites (~97%) are exchanged. The exchange of non-acidic silanol groups is very limited. The spectra of the deuterroxyl region in Fig. S1b confirm these results. Exchange at higher temperature does not lead to a further growth of the bands due to Bronsted acid hydroxyl groups.

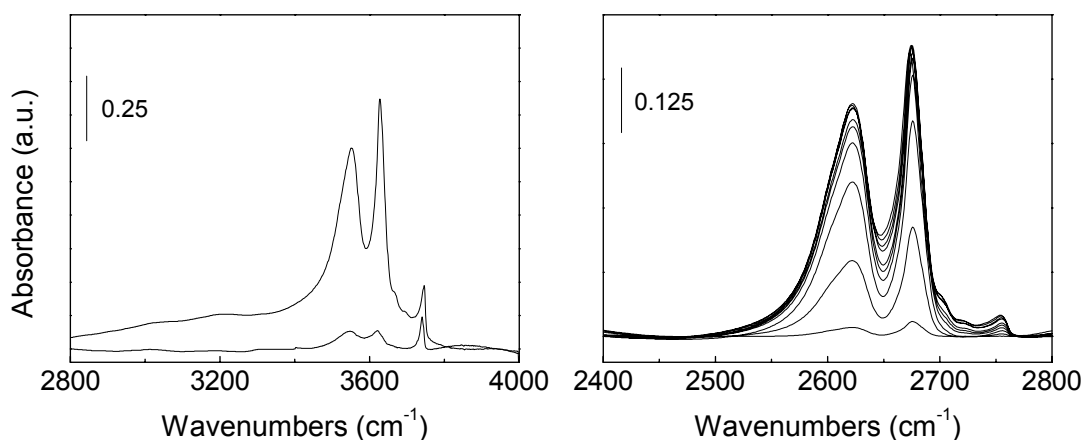


Figure S1. FTIR spectra of (left) hydroxyl region of dehydrated USY(9.6) before H/D exchange and after progressive H/D exchange at 323 K and (right) during progressive H/D exchange up to and including 523 K.

To determine the Brønsted acid concentration from the amount of deuterroxyl groups, we first calculated the concentration of Brønsted acid sites from the hydroxyl region of the parent spectrum and then from the deuterroxyl region of infrared spectra after progressive H/D exchange. Quantification from the hydroxyl group's intensities is only possible for a zeolite that is devoid of extraframework aluminium-containing phases, because otherwise other hydroxyl groups of weaker acidity in the region 3540-3670 cm⁻¹ overlap with the bands belonging to the strong acid sites.^[4] The (HF)OH band of the spectrum of dehydrated USY(9.6) can be fitted by a mixed Gaussian/Lorentzian peak. Fitting of the (LF)OH band by typical IR peak shapes was not successful. As the broad tailing (LF)OH band derives from a distribution of hydroxyl groups with an increasing degree of hydrogen bonding to the zeolite oxygen anions,^[5] we used a function to simulate such a distribution of Gaussian peak shapes, i.e.

$$G(\nu, \nu_i) = \frac{1}{\sqrt{\pi}} e^{\left[\frac{-(\nu - \nu_i)^2}{2a_0^2} \cdot \frac{1}{(1+a_1(\nu_0 - \nu_i))} \right]} \quad (1),$$

in which a_0 is the width of the Gaussian present at a base frequency ν_0 . For Gaussians generated at a frequency ν_i different from ν_0 , the peak width changes with a factor $(1+a_1(\nu_0 - \nu_i))$. These Gaussians become wider for $\nu_i < \nu_0$, which simulates the increasing line broadening upon perturbation of the hydroxyl groups by oxygen anions. The intensity as a function of the wavenumber follows from the integration of the function $G(\nu, \nu_i)$ for all Gaussians via

$$I(\nu) = \int_{\nu_0}^0 -G(\nu, \nu_i) \cdot a_2 \cdot e^{\left[\frac{-\nu_0 - \nu_i}{a_3} \right]} \cdot d\nu_i \quad (2).$$

The function $G(\nu, \nu_i)$ is weighted with an exponentially decaying function to account for the decreasing contribution of hydroxyl groups at lower frequencies with a decay constant $1/a_3$ (equivalent to a Boltzmann distribution). a_2 is a normalization factor. This function was implemented in a Levenberg-Marquardt non-linear minimization algorithm for peak fitting. Every iteration step involved the computation of the integral in equation 2. The analytic peak area is obtained by integration of $I(\nu)$ over all frequencies. The approach allowed for the simultaneous use of other peak functions. The concentrations of the various hydroxyl

components were then calculated from the areas of the peak contributions by Beer-Lambert's law employing

$$N = \frac{A}{\varepsilon \cdot \rho} \quad (3),$$

in which N is the concentration of the vibrating species ($\mu\text{mol g}^{-1}$), A is the intensity of the band (cm^{-1}), ε is the extinction coefficient ($\text{cm } \mu\text{mol}^{-1}$) and ρ is the wafer thickness (g cm^{-2}). In order to calculate the wafer thickness, the sample weight was corrected for the amount of physisorbed water. As outlined by Makarova et al., the (LF)OH band can be interpreted as a perturbed (HF)OH band caused by the interaction of the hydroxyl group with the oxygen anions in the sodalite cage. The extinction coefficient of a perturbed band depends on the frequency shift compared to the unperturbed band for the high-silica zeolite HZSM-5 via

$$\varepsilon_{(\text{LF})\text{OH}} = (1 + 0.018 \cdot \Delta\nu_{\text{OH}}) \cdot \varepsilon_{(\text{HF})\text{OH}} \quad (4),$$

which allows to calculate the molar extinction coefficient of the (LF)OH groups. $\Delta\nu$ is the frequency shift between the two bands (cm^{-1}). The extinction coefficient of the (HF)OH groups was determined in such way that the total amount of Brønsted acid protons, $N_{(\text{HF})\text{OH}} + N_{(\text{LF})\text{OH}}$, equals 2.78 mmol g^{-1} . This latter value is the concentration of Brønsted acid sites based on the amount of tetrahedral Al. The molar extinction coefficient for (HF)OH is $\varepsilon_{(\text{HF})\text{OH}} = 2.9 \text{ cm } \mu\text{mol}^{-1}$ which corresponds well to the extinction coefficient reported in literature.^[5]

Estimating the Brønsted acid density of other aluminosilicas involved the deconvolution of the deuterroxyl region of the IR spectrum after exchange at 323 K. Typically, the peak fit function consisting of a distribution of Gaussian peak shapes was used for USY zeolites and the clay. Fitting the ASA spectra was more complex and most often a Gaussian peak shape had to be included. This probably relates to the less defined structure of the acid sites in amorphous silica-alumina than in crystalline zeolite.

4. Hydroconversion of *n*-heptane

The concentration of strong Brønsted acid sites in the aluminosilicates was evaluated from catalytic activity measurements in the hydroconversion of *n*-heptane of Pd-loaded aluminosilicates. The dried aluminosilica support was shaped in a sieve fraction (177-420 μm) and loaded with 0.4 wt% Pd via incipient wetness impregnation with a solution of appropriate concentration of $\text{Pd}(\text{NH}_3)_4(\text{NO}_3)_2$. The resulting materials were calcined at 573 K. Prior to testing, the catalysts were reduced at 713 K at 30 bar in flowing hydrogen.

Hydroconversion of *n*-heptane was carried out at 30 bar at a H₂/hydrocarbon ratio of 24 mol/mol. The reaction temperature was lowered from 713 K till 473 K at a rate of 0.2 K/min. The kinetics of bifunctional, aluminosilicate-catalyzed hydroisomerization of *n*-alkanes is well understood.^[6,7] *n*-Heptane hydroisomerization involves the dehydrogenation of *n*-heptane by the noble metal phase, isomerization by strong Brønsted acid sites and hydrogenation of the *i*-olefins to *i*-heptanes. The extent of hydrocracking is limited at the conversions at which the conversion of the catalysts were compared. Meeting the requirement of sufficient hydrogenation activity is easily met if the metal loading is not too low (Figure S2). In such case, the Brønsted-acid catalyzed isomerization step of the intermediate olefins via carbenium-ion chemistry is rate limiting and the catalytic activity scales with the density of acid sites if their acidity is assumed to be constant. The activity of the catalyst is expressed as the temperature at which a hydrocarbon conversion of 40 % was achieved. Hydroisomerisation/hydrocracking of *n*-heptane is a first order reaction. From the temperature required to obtain 40% conversion, relative values for the rate constant *k* for two catalysts at a reference temperature T_{ref} can be determined using the expression

$$\ln(k_1/k_2) = E_a/R(1/T_{40,1} - 1/T_{\text{ref}}) - E_a/R(1/T_{40,2} - 1/T_{\text{ref}}) \quad (5)$$

or, if we choose the second catalyst as the reference (in Fig. 3 the USY zeolite with SAR = 8.1 is the reference) T_{ref} = T_{40,2}:

$$\ln(k/k_{\text{ref}}) = E_a/R(1/T_{40} - 1/T_{40,\text{ref}}) \quad (6)$$

in which E_a is the activation energy (kJ mol⁻¹) and R (kJ mol⁻¹ K⁻¹).

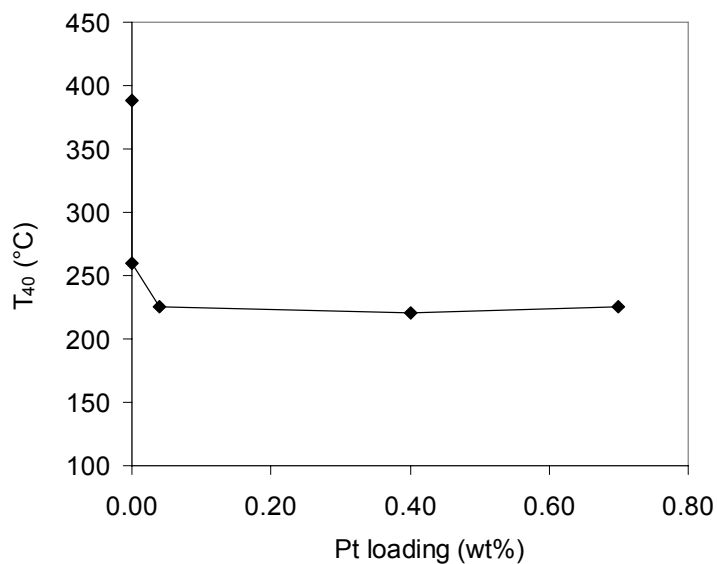


Figure S2. Catalytic activity (expressed as the temperature to obtain 40% *n*-heptane conversion) for Pt-loaded ultrastabilized Y zeolite as a function of the Pt content. A zeolite Y catalyst is loaded with 0, 0.0004, 0.04, 0.4 and 0.7 wt% Pt. The differences between Pt and Pd loaded catalysts are minor.

5. Results

The results in Table S1 and S2 correspond to the concentration of Brønsted acid sites and acid activity of the ASAs, zeolites and clays shown in Fig. 3.

Table S1. Concentration of Brønsted acid sites of a set of amorphous silica-aluminas determined by the H/D exchange FTIR method (final exchange temperature and time are 323 K and 30 min, respectively) and catalytic activities of palladium-loaded supports in *n*-heptane hydroconversion.

Sample	$N_{\text{acid sites}}$ ($\mu\text{mol g}^{-1}$)	T_{40} (K) ¹	E_a (kJ mol ⁻¹) ²
ASA(5/95, 773)	1.6	630	132
ASA(10/90, 773)	2.3	630	125
ASA(15/85, 773)	2.0	625	129
ASA(20/80, 773)	3.3	626	136
ASA(5/95, 1073)	2.6	616	130
ASA(10/90, 1073)	3.4	618	127
ASA(15/85, 1073)	6.1	604	128
ASA(20/80, 1073)	4.0	611	127

¹ Accuracy in T_{40} estimated ± 2 K; ² Accuracy in E_a estimated ± 5 kJ/mol.

Table S2. Concentration of Brønsted acid sites of a set of USY zeolites and clays determined by the H/D exchange FTIR method (final exchange temperature and time are 323 K and 30 min, respectively) and catalytic activities of palladium-loaded supports in *n*-heptane hydroconversion.

Sample	$N_{\text{acid sites}}$ (mmol g ⁻¹)	T_{40} (K) ¹	E_a (kJ mol ⁻¹) ²
USY (8.1,I)	0.80	493	131
USY (8.1,II)	1.25	486	130
USY (9.3)	0.27	506	128
VUSY (26.5)	0.52	499	143
VUSY (33.1)	0.23	508	137
XVUSY (70)	0.29	536	146
XVUSY (85)	0.13	563	146
Mg-SAP(13)	0.012	555	132

¹ Accuracy in T_{40} estimated ± 2 K; ² Accuracy in E_a estimated ± 5 kJ/mol.

Fig. S3 shows the hydroxyl region of the IR spectrum of ASA(5/95, 1073) before and after progressive H/D exchange at 323 K and 1800 s. Clearly, the extent of H/D exchange of silanols is very limited (below 1%). Fig. S4 shows the OD part of the IR spectra of ASA(5/95, 1073) and Na-ASA(5/95, 1073) after progressive H/D exchange at 323 K and 1800 s. This result indicates that H/D exchange of the silanol groups is absent after exchange of the acidic surface hydroxyl groups. Thus, the exchange of the silanol groups is a secondary process involving the surface H/D exchange between acidic OD groups and nearby silanol groups or is due to trace amounts of water. A similar result was obtained after Na^+ exchange of a VUSY zeolite.

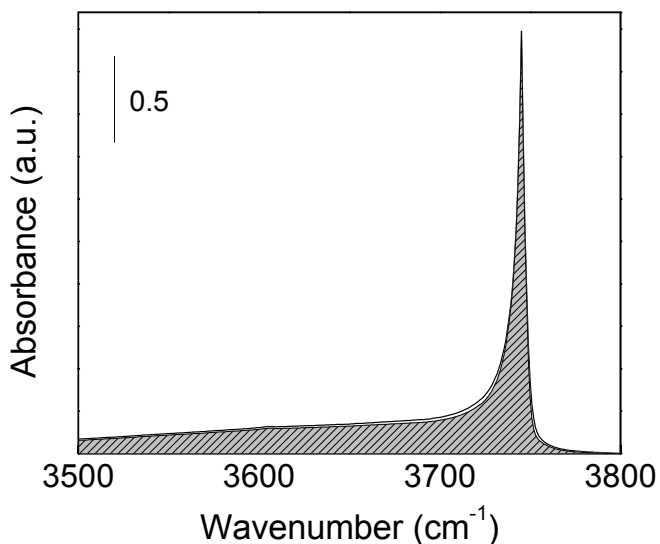


Figure S3. Infrared spectrum of the OH region of an ASA with a nominal Al_2O_3 content of 5 wt% before and after (filled area) progressive H/D exchange at 323 K and 1800 s.

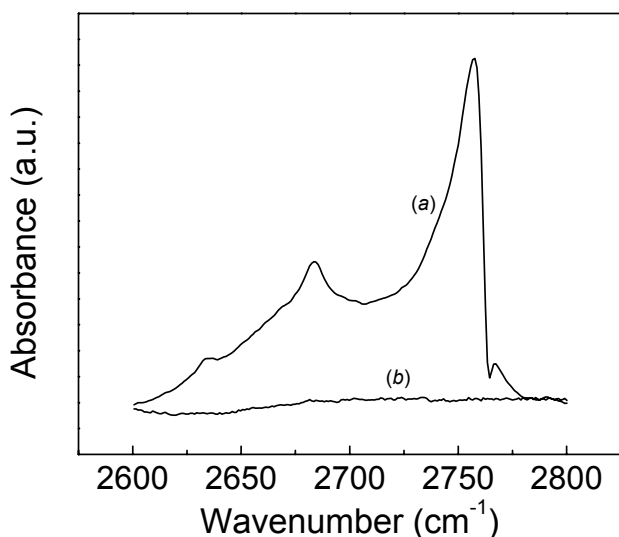


Figure S4. Infrared spectrum of the OD region after progressive H/D exchange at 323 K and 1800 s of ASA(5/95, 1073) and a Na^+ -exchanged ASA(5/95, 1073).

References

1. US Patent 4503023, 1985.
2. R. J. M. J. Vogels, J. T. Kloprogge, J. W. Geus, *Am. Mineral.*, 2005, **90**, 931.
3. E.J.M. Hensen, D.G. Poduval, P.C.M.M. Magusin, A.E. Coumans, R.A. van Santen, *J. Catal.*, 2010, **269**, 201.
4. M. A. Makarova, J. Dwyer, *J. Phys. Chem.*, 1993, **97**, 6337.
5. M. A. Makarova, A. F. Ojo, K. Karim, M. Hunger, J. Dwyer, *J. Phys. Chem.*, 1994, **98**, 3620.
6. G. E. Gianetto, G. R. Perot, M. R. Guisnet, *Ind. Eng. Chem. Prod. Res. Dev.*, 1986, **25**, 481.
7. J. W. Thybaut, C. S. Laxmi Narasimhan, J. F. Denayer, G. V. Baron, P. A. Jacobs, J. A. Martens, G. B. Marin, *Ind. Eng. Chem. Res.*, 2005, **44**, 5159.